

ROTOR TIP STALL FROM A DESIGNER'S PERSPECTIVE

A. Schneider – A. Silingardi – P. Astrua – E. Puppo – S. Depalo

Ansaldo Energia
Via N. Lorenzi, 8, 16152, Genova, Italy
Andrea.Schneider@ansaldoenergia.com

ABSTRACT

The operating range of a compressor is the most critical aspect to consider when dealing with new designs. Two distinct routes to compressor stall are known in literature: modal-stall that occurs near the peak of the overall characteristic and spike-stall that initiates on the negatively-sloped part of the characteristic curve. Modal type stall can be taken into account from the very beginning during the design process. The basic mechanisms that drive the phenomena are essentially 2D in nature and there are well-established and experimentally validated design criteria available. Unfortunately this statement no longer applies when dealing with spike-type stall. This short length-scale instability is related to a three-dimensional breakdown of the flow that appears at rotor tip.

Since when firstly observed, much effort has been expended trying to understand the flow features underlying this abrupt stall. Nevertheless, a well-established and validated design criterion is still missing.

This paper deals with the topic from a designer's perspective. A discussion which tries to highlight the design variables affecting the spike-stall is presented in the first part of the paper. Then CFD results on core stages of an heavy-duty axial compressor are discussed. The aim is to derive useful considerations for the designer work and discuss which design actions are more effective to successfully complete a spike-stall safe design.

KEYWORDS

COMPRESSOR, DESIGN, SPIKE STALL, SURGE

NOMENCLATURE

c_x	Axial velocity
CFD	Computational Fluid Dynamics
DF	Diffusion Factor of Lieblein
LER	Leading Edge Recambering
L.E.	Leading Edge
M	Mass flow rate
PR	Total to Total Pressure Ratio
RANS	steady Reynolds Averaged Navier Stokes equations
T.E.	Trailing Edge
TF	Throughflow code
URANS	unsteady Reynolds Averaged Navier Stokes equations
TM	Turbulence Model
u	Peripheral rotational speed

Greek symbols

ϕ	Phi: flow coefficient $\frac{c_x}{u}$
--------	---------------------------------------

INTRODUCTION

Spike-stall owes its name to the spike-like appearance of the disturbance recorded on the velocity traces during the stall inception. Since when firstly reported (Day [1], 1993) much effort has been expended trying to understand the path that leads to this type of stall inception. A comprehensive paper review of the large amount of work on this topic is given in Tan et al. [6], (2010). In spite of this effort this type of stall inception remains critical from design standpoint for several reasons. Contrary to modal-type stall, precursor activities are very hard to detect. During full scale operation on a test bed there are very few chances to test the stall margin related to such stall mechanism without possibly damage the prototype. From design-tool point of view, the modelling is difficult at least for two reasons. The first is that is related to locally-confined three-dimensional flow breakdown. Furthermore this inception mechanism is affected by design variables hard to predict in the early design stage (e.g. tip clearance gap and end-wall blockage).

The organization of the paper is as follow. First a brief description of the spike-stall flow features is presented. Following that, a discussion regarding the design variables affecting the spike-stall tendency of an heavy-duty axial compressor is made. Then we present CFD computations on a set of systematic series of configurations, whose aim is to develop useful consideration from a designer's perspective.

SPIKE-STALL FLOW FEATURES

A vast literature is available regarding the flow features of spike-stall. The research community generally agree on the following:

- ✓ The phenomenon is localized at the tip region of a rotor row.
- ✓ It is an instability with short length scale (several blade pitches) that propagates around the annulus quicker than modal oscillations.
- ✓ Contrary to modal-type, there is no precursor. After the spike first appears, a stall cell is developed in few rotor revolutions.

One early relevant work on this topic (Camp and Day [7], 1998) has introduced the concept of critical rotor incidence. Based on a set of test rig experiments, it has been shown that the stability limit is set by the incidence at rotor tip. After this work, much effort has been expended over the past years by the scientific community trying to understand the physical features that underlies the spike-stall. Up to now, two different flow features and mechanisms has been identified, both experimentally and numerically:

- Forward spillage and trailing edge backflow.
- Tornado-like vortex.

Forward spillage mechanism

According to Vo [2], (2005), the forward spillage criterion sets the condition for the spike formation. This criterion takes into account the interaction between the tip leakage flow and the incoming flow. Experimental and numerical evidences of several works show that the spike-stall initiates when the interface between incoming/tip-clearance flows is aligned with the rotor leading-edge plane. In this condition the leakage flow spills forward of the adjacent blade. Another condition required for spike inception is that the flow from tip-clearance region of one blade moves across the blade passage of the adjacent one by passing around T.E. This gives origin to a backflow that impinges on the pressure side and increases its pressure, thus generating a higher blockage (Vo [2], 2005, Bennington et al. [4], 2010 and Deppe et al. [5], 2005). A sketch that explains the basic flow features related to this criterion is shown in Figure 1 (left). A very effective and simple way to detect the occurrence of the forward spillage and T.E. backflow is to plot the sign of axial velocity in a blade-to-blade plane near the rotor tip. The interface between incoming/tip-clearance flow is the locus where the axial velocity changes its sign. The forward-spillage occurs when this interface is upstream the L.E. plane. The T.E. backflow is present when the axial velocity is negative in some portion of the T.E. outlet plane (yellow dashed line in Figure 1, left).

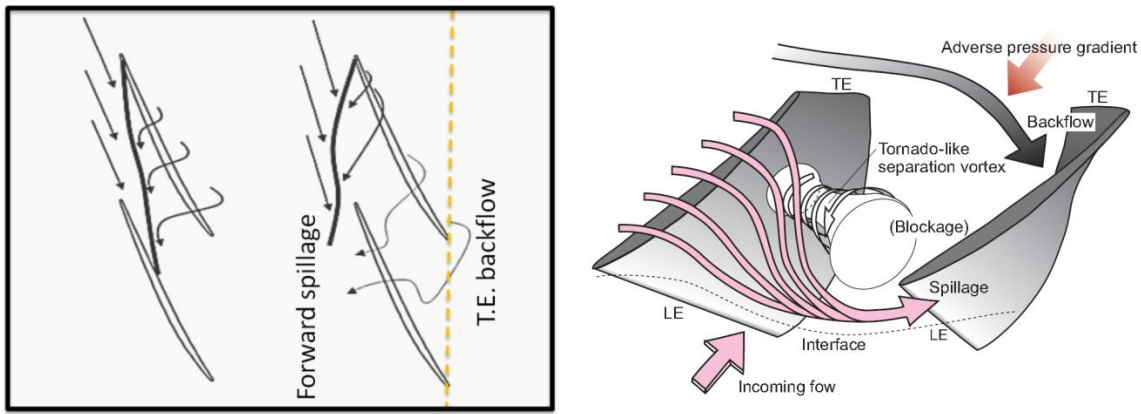


Figure 1. Illustration of forward-spillage criterion (left, Bennington, 2010), and tornado-like separation vortex (right, Yamada et al. 2012)

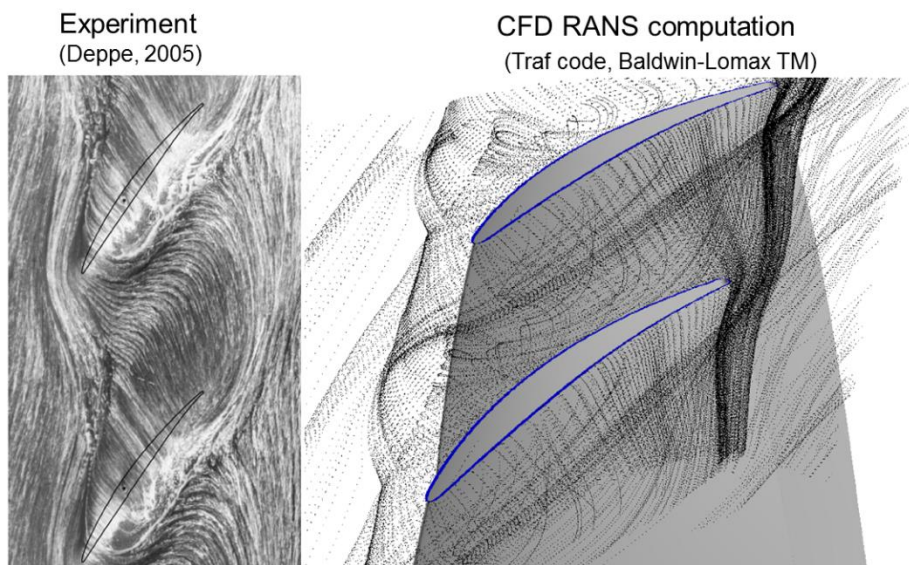


Figure 2. Forward-spillage and T.E. impingement flow features: on the left experiments (from Deppe et al. 2005 [5]) and on the right a near stall condition from a computation done for the present work.

Tornado-like vortex

Since the spike-stall has been reported also on shrouded blades (without tip gap) and in centrifugal compressor vaned diffuser, it is clear that the forward spillage criterion cannot be exhaustive on the matter. More recently, another criterion, initially suggested by März et al. [15], (2002), has been investigated in details by Inoue et al. [8], (2000) and Yamada et al. [9], (2012). The cited works show that the spike appearance is linked to the formation of a tornado-like separation vortex resulting from a leading edge separation near the rotor tip. A basic sketch explaining the flow features related to this criterion is shown in Figure 1 (Yamada, 2012).

DESIGN VARIABLES AFFECTING THE SPIKE-STALL

A conceptual framework that could be exploited to derive useful design considerations when tip clearance is present, is discussed in Bennington et al. [4] (2010). According to their work, the interface between the main flow and the tip leakage flow can be effectively defined by the locus where the axial velocity reverses its sign. They also observe that the axial position of the interface is determined by a momentum balance in the axial direction between the incoming flow and the tip leakage flow. By looking at tip axial velocity, the forward-spillage criterion is reached when the

interface moves upstream of the L.E. plane. The T.E. backflow is reached if the axial velocity is negative in some portion of the T.E. outlet plane. With the above concept in mind, the design variables that could in principle affect the forward spillage criterion are:

- Blade loading: high blade loading increases the pressure drop across the tip gap and thus the leaked flow momentum.
- Tip gap: greater gap implies greater leaked flow momentum.
- Stagger angle: the stagger angle determines the axial component of the clearance leaked flow (higher stagger angle means greater axial component).
- Aerofoil curvature distribution determine the front-aft loading that affect the tip-vortex structure.
- Bleeds and/or inlet distortion: local defect in flow axial momentum can promote forward-spillage on downstream rotor.

TOWARDS A SAFER DESIGN

Early design stage

In the initial design stage, decisions that are likely to determine whether the project will succeed or fail have to be made. Unfortunately this is also the stage where some important information is still missing. Some of these choices are very difficult to change in later design phases. One of them is the meridional channel passage area. The passage area, contributes to determine the flow coefficient. According to the concept of forward spillage and T.E. backflow, the flow coefficient which is basically proportional to the axial flow momentum, together with tip blade loading and tip-clearance dimensions, may have a significant impact on spike-stall margin. The strong impact of tip-clearances on stall margin is widely reported in literature ([21],[22]). It should be also pointed out that rubbing during transient operation could lead to increased tip gap, and that this increase is difficult to predict during the preliminary design phase. Furthermore, casing bleeds may induce relevant distortion of flow coefficient near the tip of the downstream blade. This distortion is locally confined and most likely not accurately predicted by Throughflow codes. Another remarkable observation is that widely spaced blade rows promote localized spike-type disturbance (Tan et al. [6], 2010). Widely spaced rows are usually linked to the presence of bleeds, and again this feature is not usually taken into account by TF codes. For all the above reasons, it may be safe to set a minimum flow coefficient at tip during the design of meridional passage area, regardless of what TF tool would suggest as an optimum solution.

Another design features that should be carefully evaluated is the flow coefficient span-wise gradient, which could be seen as a design variables that determines the hub/tip relative stall tendency. An interesting discussion is given in Simpson and Longley [11] (2007). Their experimental work showed that is possible to switch from modal to spike stall through a span-wise redistribution of flow coefficient.

Final design phase

Let's now assume to have frozen the meridional design (stage loading, meridional passage area, row-by-row inlet and outlet radial variation of all thermodynamic quantities) and that during the final design phase it is found that stall-margin is limited by spike-type inception on some rotor tip. What kind of actions can the designer put in place to increase the stall margin at this design phase?

The golden rule would be to increase the flow coefficient in the upstream near-casing section of the stalled rotor. To this aim, the energy exchange at tip should be increased in the upstream section.

Unfortunately there are few chances of increasing the mass flow that evolves through tip sections without changing the meridional design. Nevertheless is still possible to use some 3D design feature (e.g. end-bending of vanes) to locally increase the axial velocity by reducing

secondary flows. In the next sections this and other design options suitable for the final design stages are taken into account. The effectiveness of these actions are discussed by means of CFD computations.

CFD COMPUTATIONS

The first problem every designer has to deal with is to choose the simplest yet adequate tool depending on specific design task. As far as the spike-type stall inception is concerned, the complete resolution of the path towards stall requires time-accurate computations (URANS). However there is evidence in literature that a single passage, steady, RANS computation can be used to estimate the limit of steady operation, and thus check the width of the stall margin (Hoying [10], 1999, Vo [2], 2005). There are also a large number of papers pointing out the difficulty to evaluate accurately the stability limit with a steady RANS approach. In addition to that, it is known that compressors can deal with unsteady flows before surge. However for the purpose of the present paper it is enough to have a qualitative/relative tendency of the effect of design modifications on the stability limit. For these reasons steady computations have been used for the present work and there will be no information related to the unsteady flow structures after the first instability appears. The CFD setup used is described in the appendix.

With respect to the experimental approach, CFD allows to easily separate the contribution of each design variables. In spite of the uncertainty of CFD capability to correctly compute the absolute value of stall margin, in relative and qualitative terms, the numerical approach can be effectively exploited to derive useful consideration from designer point of view. An heavy-duty axial compressor has been used as a test case. In Figure 3 (left) two speed-lines computed through CFD multi-stage RANS computations are shown. The low speed characteristic (N95, 95% reduced speed) has been chosen because it exhibits a numerical stall at 9th rotor tip. By looking more in details, it has been found that the region where the flow breakdown appears (judged in terms of outlet axial velocity deficit) is located in the upper 15-20% of blade height. In the following sections CFD results on a series of geometrical modifications of vane 8 and rotor 9 are presented. The aim is to find an effective way to increase the stall margin of the stage 9, and to increase the stability limit of the whole compressor.

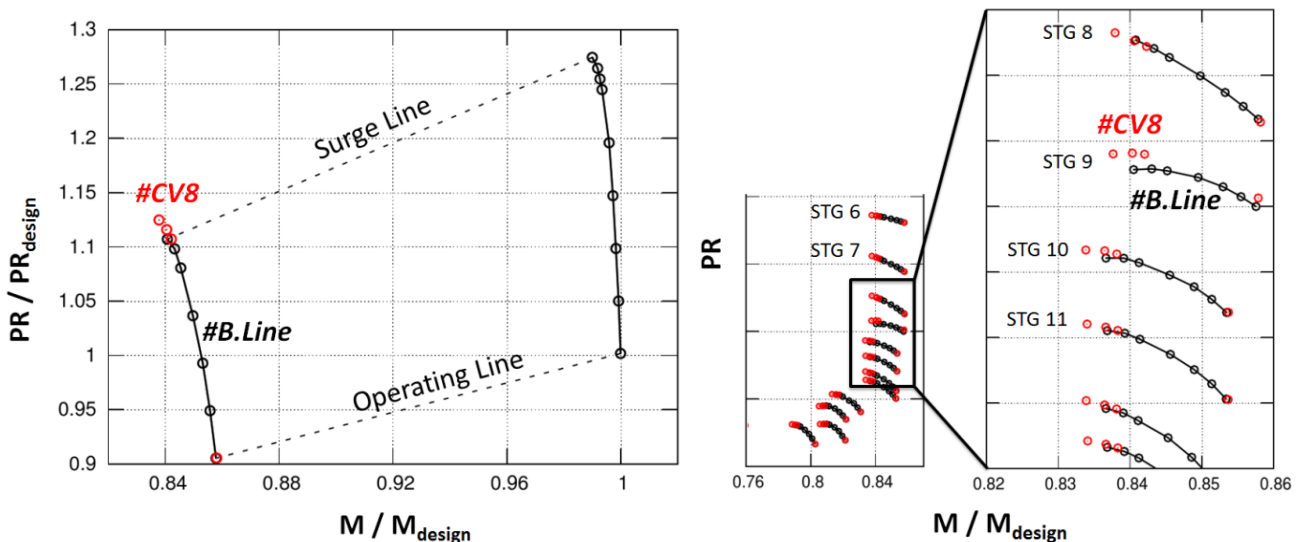


Figure 3: Left: Overall characteristic of the compressor in design and low speed (N95, 95%) conditions. Right: stage by stage characteristic curves

Vane 8 redesign

By looking more in details the flow features at near stall condition, a significant corner separation at the vane 8 tip is found. In order to reduce such separation, the vane 8 has been redesigned by applying a simple 3D stacking of the aerofoils, similar to the one described in

Gallimore et al. [3] (2002). This redesign will be referred as #CV8. An illustration of the redesign is shown in Figure 4 (left). In Figure 3 are shown respectively the overall (left) and stage-by-stage characteristics (right) of the baseline (#B.Line) and redesign (#CV8) configurations. Surprisingly, a locally confined redesign of a single row leads to a significant increase in stability margin of the whole compressor. This can be explained by looking at the stall mechanism. The reduction of the secondary flows induces a flow coefficient increase on tip region (roughly 2% over the upper 10% span) of the downstream rotor, which is the most critical for that operating condition. From the characteristic of stage 9 (Figure 3) it can be seen that this span-wise mass flow redistribution delay the rotor 9 stall and enables a pressure ratio recovery of stage 10 (and to a less extent 11, 12 and 13). In Figure 4 (right) a meridional view of the channel is shown. The coloured map reports the axial velocity percentage difference with respect to the #B-Line case. It can be noted how the redesigned stator increases the axial velocity in the tip clearance region of blade 9 and 10.

Vane 8 tip re-stagger

To further investigate the influence of vane 8 outlet conditions on rotor 9 stall inception mechanism, two additional designs have been produced. These designs have been built by restaggering the 8th vane by +/- 4 degrees at tip (linearly decreasing to zero towards the hub). These two additional configurations will be referred as #CV8+4 and #CV8-4. In order to ensure that the stall inception doesn't move to another stage when throttling the whole compressor, all tip clearances have been closed, except the one of the rotor 9, which has been settled to a value of 2.5% of the tip chord. The objective is to see how the relative inlet flow angle and inlet flow coefficient affect the stall inception of the rotor 9. In the Figure 5 (right) the characteristic curve of the tip section of the rotor 9 (at 85% span) is reported, while on the left a similar curve where the inlet relative flow angle replaces the flow coefficient is shown. Interestingly, the inlet relative flow angle correlates better with stall inception than flow coefficient. This finding is in accordance with the observation made by Camp and Day [7] (1998). An extended experimental campaign was conducted on Cambridge low-speed research compressor. Similarly to the presented CFD computations, the stagger of regulating vanes were varied to see the effect on a fixed geometry rotor. Based on their work, Camp and Day suggested that the spike-stall occurs when a limiting value of tip rotor incidence is reached. In this particular case the inlet flow angle limiting value is about -70 degrees. This value, for the three cases, is reached with 3 different combinations of flow coefficients and absolute flow angles.

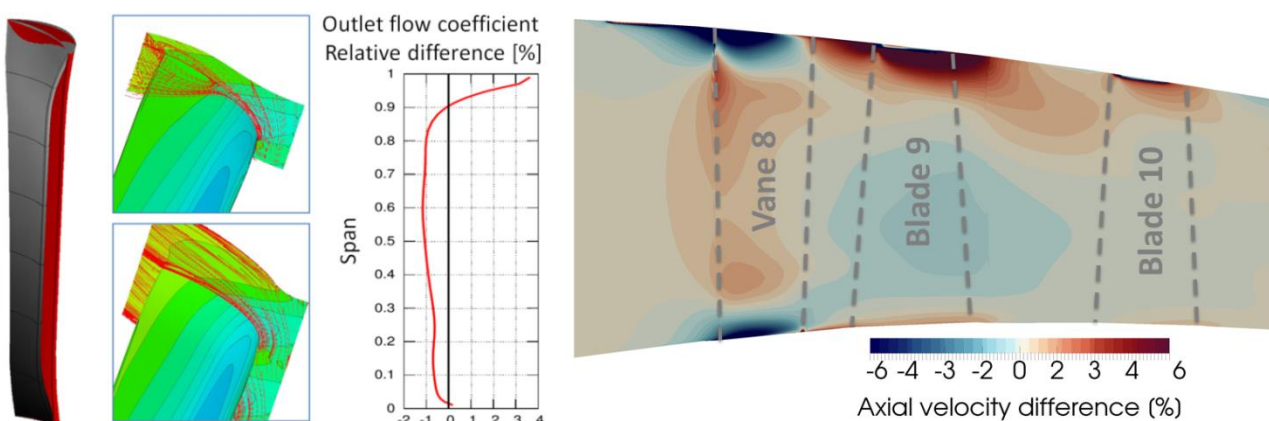


Figure 4: Left: #CV8 redesign (grey blade), resulting corner stall reduction and outlet flow coefficient variation. Right: Tangentially-averaged axial velocity variation between baseline and #CV8 redesign at N95 operating line

Because of the lower inlet velocity, the 9th stage of the #CV8+4 configuration delivers lower outlet pressure, but its operating range extend towards lower mass flow rates, thus allowing the overall characteristic to reach higher pressure ratio (see Figure 6, left).

In Figure 6 on the right a coloured map of axial velocity sign is shown, where the backflow (negative axial velocity) is painted in blue. The measure plane is placed exactly at blade tip. The aim is to evaluate the forward spillage and the T.E. backflow criteria. In the first row the operating line condition for each of the three configurations is shown.

In the second row, the near-stall condition (each configuration throttled to its limiting backpressure), while in the third row an operating condition with the same backpressure (corresponding to the near-stall condition of the #CV8-4 configuration) is shown.

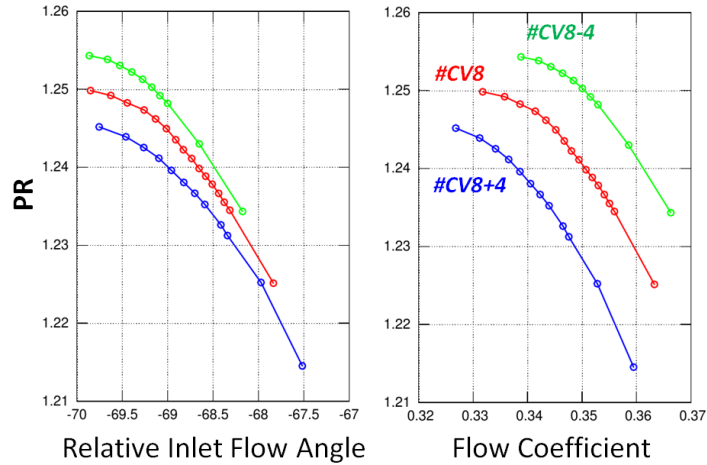


Figure 5: Rotor 9 tip section (85% span) characteristic curves

As far as forward spillage criterion is concerned, the spillage is present even at operating line conditions. This flow feature may be promoted by the high stagger angle of the actual rotor which implicates high axial component of the tip leakage flow momentum. Interestingly, the T.E. backflow criterion and the general appearance of the axial velocity sign plot correlates quite good at stall points. It can be seen that the backflow region is pretty similar for the three configurations at near-stall condition, as well as the axial position of the incoming/tip-leakage flows interface near L.E..

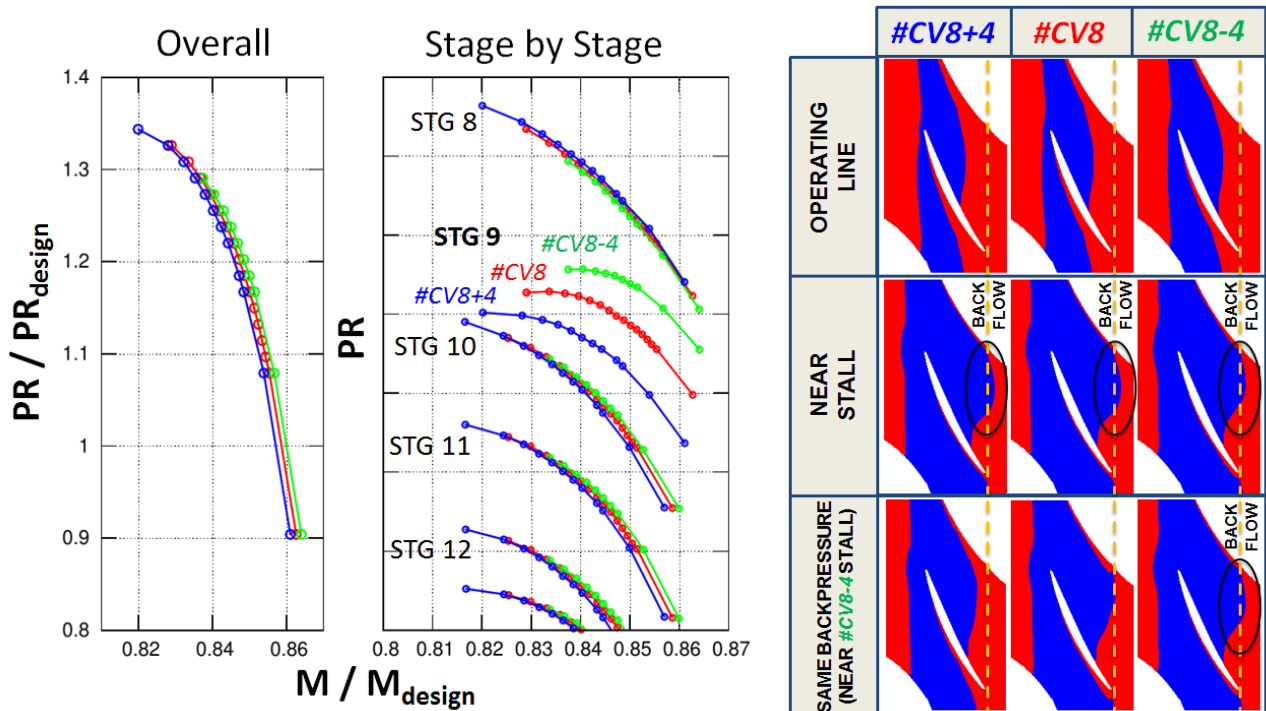


Figure 6. Left: Overall and stage-by-stage characteristics. Right: Axial velocity at rotor 9 tip. Forward (red) and reverse flow (blue).

It should be noted that at stall conditions the configurations show different flow coefficient at tip (Figure 5, graph on the right). Since the interfaces between incoming/tip-leakage flows are determined by a momentum balance, this means that the configuration with lower inlet flow coefficient must have a weaker tip-leakage flow momentum. The blade loading at stall in terms of pressure ratio is in fact lower (Figure 5, left).

To summarize, the following observations can be drawn:

1. The stall initiates when a limiting value of inlet relative flow angle is reached at the tip of the rotor. This relative angle can be obtained with lower flow coefficient and higher absolute angle or vice versa.
2. When this limiting relative angle is reached, the tip-clearance flow structure, in terms of forward spillage and T.E. backflow, is similar for the three cases analysed. This can be explained by thinking at a simple momentum balance between incoming/tip-leakage flows. When the incoming flow momentum is lower, also the tip-leakage flow momentum is lower due to the lower blade loading.

Rotor 9, Leading Edge Recambering and increased solidity

The last three configurations presented have been obtained by varying rotor 9, while vane 8 has been kept fixed. For the sake of clarity, a summary of all tested configurations is reported in Table 1. The configuration #CV8 will be the baseline of this series of modifications. The first configuration has been obtained by applying a Leading Edge Recambering aimed at increasing the aerofoil inlet metal angle by 6 degrees. This is a typical intervention that designers adopts to address problems of high incidence. The stagger angle has been slightly adjusted (about 0.5 degrees) in order to keep the pressure ratio unchanged at operating point. This configuration will be referred as #CB9_LER.

The second and third configurations have been designed in order to increase the tip solidity by means of two different actions: increasing the blade count and increasing the aerofoils chord at tip. Again a small re-stagger has been applied to keep the pressure ratio nearly constant at operating point. The solidity at tip has been increased by about 14% for both cases. This two configurations will be referred as #CB9_BLC (rotor 9 Blade Count increased) and #CB9_CHD (rotor 9 tip Chord increased). The chord of #CB9_CHD case has been linearly increased towards the tip. The hub chord has been kept constant. The stacking line is barycentric, therefore no lean or sweep has been induced.

	#CV8	#CV8+4	#CV8-4	#CB9_LER	#CB9_BLC	#CB9_CHD
Vane 8, lean	Yes	Yes	Yes	Yes	Yes	Yes
Vane 8, tip re-stagger	0	+4	-4	0	0	0
Rotor 9, tip L.E.R.	0	0	0	+6	0	0
Rotor 9, blade count	/	/	/	/	+10	/
Rotor 9, tip chord	/	/	/	/	/	+18%
Rotor 9, Solidity at 85% span	/	/	/	/	+14%	+14%
DF at 85% span	0.416	0.41	0.422	0.41	0.395	0.40
Tip gap/chord	2.5%	2.5%	2.5%	2.5%	2.5%	2.1%

Table 1: Summary of tested configurations.

The first observation that has to be made is that in this case the value of critical incidence may be different for each of the new configurations. In fact, contrary to the series presented in the previous section, the geometry of the rotor 9 has been changed. A second observation is that since

the vane 8 and thus the absolute flow angle is fixed, the relative flow angle is a function of flow coefficient only, and this is the reason why the two graphs of Figure 7 (right) looks similar.

Going to the results (Figure 7) it can be noticed the following:

- ✓ #CB9_BLC shows an overall stall margin similar to the #CV8, with 9th stage reaching a peak of the characteristic slightly higher.
- ✓ #CB9_LER has a stall margin lower than #CV8. By looking at the tip section (Figure 7, right), a slightly lower flow coefficient (and relative inlet flow angle) is reached with respect to #CV8. This is consistent with Leading Edge Recambering which is known to make the aerofoil more tolerant to incidence. However it can also be noted that the whole compressor stalls at higher mass flow rate (see Figure 7, left). This means that a span-wise massflow redistribution on rotor 9 has occurred. In Figure 8 (on the left) a relative difference in terms of flow coefficient from #CV8 to #CB9_LER case is shown at near-stall condition. It can be seen that a reduction of 3/4 % of flow coefficient is found in the upper part of the blade.
- ✓ #CB9_CHD shows a higher stall margin than #CV8. This is a really interesting point since, from a purely 2D point of view, the geometry at tip is similar to the #CB9_BLC. The two configurations share the same aerofoil, stagger and solidity. The differences must be due to 3D effect (e.g. tip leakage flow structure) and/or span-wise mass flow redistribution that changes the boundary conditions of the tip section. In Figure 8 (right) a meridional view of the channel is shown, The coloured map reports the axial velocity percentage difference with respect to the #CV8 case. It can be observed that already at operating line, and to a more extent at near-stall condition (left graph), there is an axial velocity redistribution towards the tip sections. The last point that should be highlighted is that due to the chord increase the ratio between tip gap and chord for this configuration is reduced from 2.5% to 2.1% (Table 1).

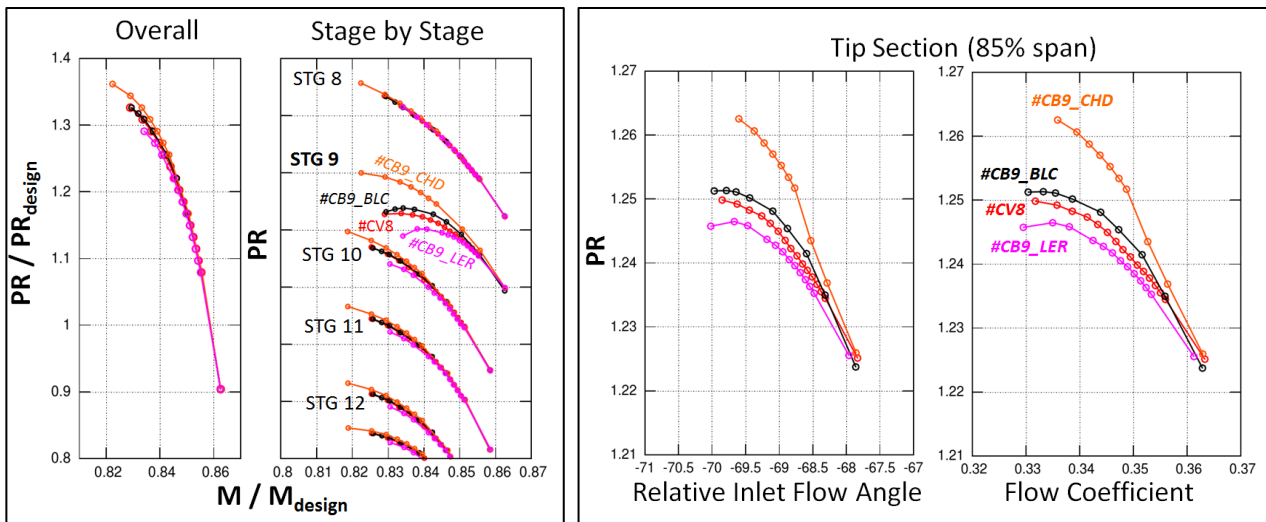


Figure 7. Left: Overall and stage-by-stage characteristics curves.

Right: Rotor 9 tip section (85% span) characteristics.

Relative difference with respect to #CV8 configuration.

As far as the forward spillage/T.E. backflow criteria is concerned, the configurations at near stall conditions are much different (see Figure 9). Both #CB9_LER and #CB9_BLC (especially the first) shows a wider region of backflow. For some reason this configurations are somehow more tolerant (at least from a numerical point of view) in terms of backflow region at tip. Contrary, the configuration with increased tip chord (#CB9_CHD) does not show T.E. backflow at stall point.

It should be also pointed out that #CB9_CHD is the only configuration that does not show forward spillage at operating line (the L.E. is in a region of positive axial velocity).

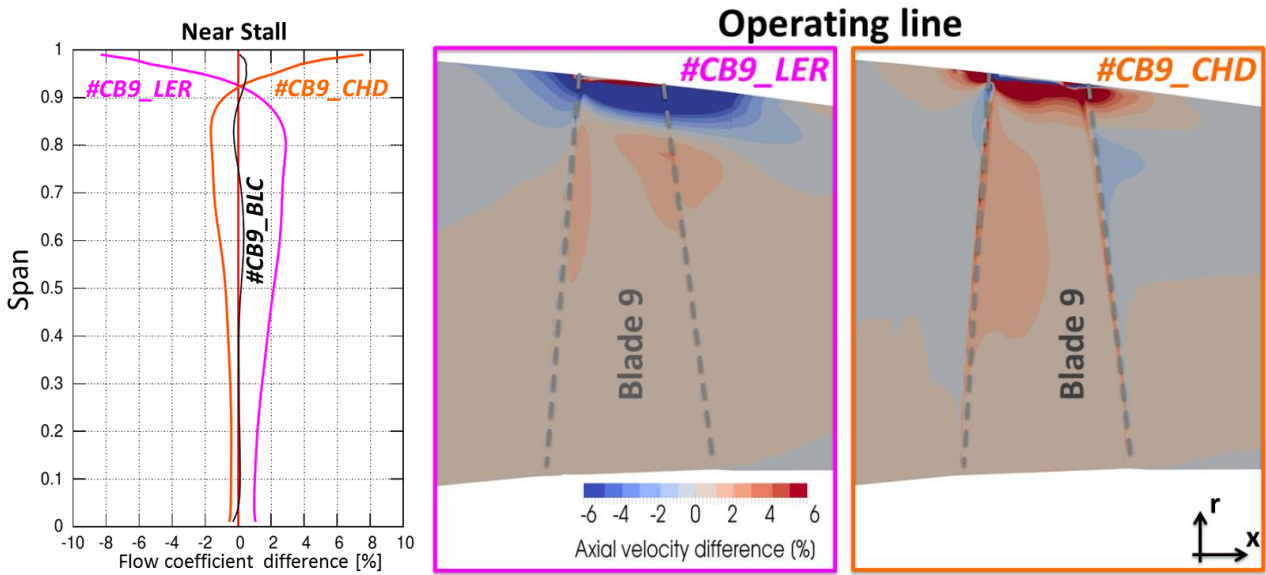


Figure 8:

Left: Variation (%) of span-wise flow coefficient with respect to #CV8 case, rotor 9 outlet, near stall condition.
 Right: Variation (%) of axial velocity between #CV8 case and redesigns (#CB9_LER and #CB9_CHD)

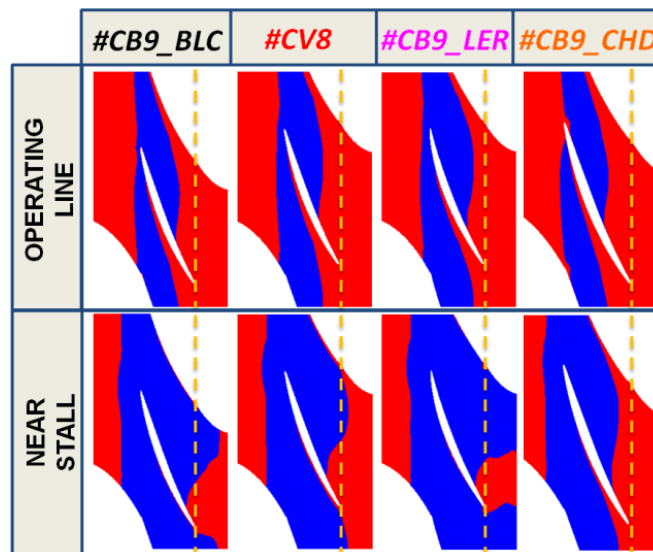


Figure 9. Axial velocity at rotor 9 tip. Forward (red) and reverse flow (blue).

To summarize the following observation can be made:

- ✓ The configuration #CB9_LER with higher inlet metal angle determines a span-wise redistribution of the flow (see Figure 8, mid plot). This redistribution determines the reduction of the flow coefficient over the last 7/8% of the blade height and anticipates the stall of the tip section, even if the aerofoils itself should be more tolerant to incidence. The consequence is a reduced stall margin of the whole compressor.
- ✓ No substantial increasing in stall margin has been found for #CB9_BLC configuration with higher blade count.
- ✓ The configuration with increased tip chord (#CB9_CHD) shows a significant increasing of stall margin. This seems related to a span-wise redistribution of mass flow towards the tip section.

- ✓ Forward spillage and T.E. backflow criteria do not correlate well with stall inception point.

It is worth observing that re-design actions that usually goes on stall margin in a purely 2D environment (e.g. Leading Edge Recambering and increased blade count) can have null or even detrimental effect if this re-designs divert the mass flow from tip towards lower sections.

Given the results, the more effective redesign to address a spike-stall issue is the one that radially redistribute the flow towards the rotor tip section.

CONCLUSIONS

Multistage CFD computations on a heavy-duty multi-stage axial compressor has been used to derive useful considerations on spike-stall from a designer point of view. The baseline compressor exhibits a spike-stall at rotor 9 tip. A series of design modifications have been applied to the upstream stator and then to the rotor itself.

Results of upstream stator modifications with rotor geometry fixed have led to the following observations:

- ✓ The stall initiates when a limiting value of inlet relative flow angle is reached at the tip of the rotor.
- ✓ Despite different flow coefficients at tip, the cases analysed showed a similar configuration in terms of forward spillage/T.E. backflow features, in accordance with the corresponding criteria as suggested in literature.

As an example, it has been shown a case where a significant increase of stall margin has been achieved by a simple redesign of the upstream stator aimed at reducing secondary flows and thus increasing the flow coefficient near the casing.

Results of rotor 9 modifications with upstream stator fixed have shown that:

- ✓ Since the absolute flow angle is fixed, it is the flow coefficient at casing that determines the rotor inlet relative flow angle and thus largely rules the stall margin.
- ✓ The more effective redesign to address a spike-stall issue is the one that radially redistribute the flow towards the rotor tip section.

Results are generally in agreement with the literature, in particular with the concept of critical rotor incidence at tip. Also the forward spillage/T.E. backflow criteria correlates well with stall-inception in case of fixed rotor. However, discrepancy on the formentioned criteria has been found on other cases. In particular it has been found that the extension and shape of tip-clearance backflow region at near-stall conditions depends on the particular rotor geometry. To the authors knowledge, this circumstance has not been previously reported in literature and further investigations would be needed.

Much knowledge has been gained on spike-stall inception during the last decades. Nevertheless, a more 'design-oriented' effort would still be necessary, being the goal the development of spike-stall design criteria to be used since early stages of design process.

ACKNOWLEDGMENT

The authors would like to thank L. Cozzi, F. Rubecchini and M. Marconcini of the University of Florence "T-Group" for the commitment and the constant effort devoted to the development of a robust and reliable numerical setup suitable for industrial design.

REFERENCES

- [1] Day, I.J., 1993, "Stall Inception in Axial Flow Compressors" ASME Journal of Turbomachinery, 115, pp.1-9
- [2] Vo, H.D., Tans, C.S., Greitzer. E.W., 2005, "Criteria for Spike Initiated Rotating Stall", ASME paper GT2005-68374

- [3] Gallimore, S.J., Bolger, J.J., Cumpsty, N.A., Taylor, M.J., Wright, P.I., Place, J.M.M., 2002, "The Use of Sweep and Dihedral in Multistage Axial Flow Compressor Blading" ASME Journal of Turbomachinery, 124, pp. 533-541
- [4] Bennington, M.A., Ross, M.H., Cameron, J.D., Morris, S.C., Du, J., Lin, F., Chen, J., 2010, "An Experimental and Computational Investigation of Tip Clearance Flow and its Impact on Stall Inception", Proceedings of ASME Turbo Expo 2010, GT2010-23516
- [5] Deppe, A., Saathoff, H., Stark, U., 2005, "Spike-Type Stall Inception in Axial-Flow Compressor" Proceedings of the 6th European Conference on Turbomachinery Fluid Dynamics and Thermodynamics, Lille, France
- [6] Tan, C.S., Day, I, Morris, S., Wadia, A, 2010, "Spike-Type Compressor Stall Inception, Detection, and Control", Annu. Rev. Fluid Mech, pp. 275-300
- [7] Camp, T.R., Day, I., 1998, "A Study of Spike and Modal Stall Phenomena in a Low-Speed Axial Compressor", ASME Journal of Turbomachinery, 120, pp. 393-401
- [8] Inoue, M., Kuroumaru, M., Tanino, T., Yoshida, S., Furukawa, M., 2000, "Comparative Studies on Short and Long Length-Scale Stall Cell Propagating in an Axial Compressor Rotor", Proceedings of ASME Turbo Expo 2000, GT2000-0425
- [9] Yamada, K., Kikuta, H., Iwakiri, K., Furukawa, M., Gunjishima, S., 2012, "An Explanation for Flow Features of Spike-Type Stall Inception in an Axial Compressor Rotor", Proceedings of ASME Turbo Expo 2012, GT2012-69186
- [10] Hoying, D.A., Tan, C.S., Greitzer, E.M., 1999, "Role of blade passage flow structures in axial compressor rotating stall inception", ASME Journal of Turbomachinery, 121, pp. 735-742
- [11] Simpson, A.K., Longley, J.P., 2007, "An Experimental Study of the Inception of Rotating Stall in a Single-Stage Low-Speed Axial Compressor", Proceedings of ASME Turbo Expo 2007, GT2007-27181
- [12] Arnone, A., 1994, "Viscous Analysis of Three-Dimensional Rotor Flow Using a Multigrid Method", ASME Journal of Turbomachinery, Vol. 116, pp. 435-445.
- [13] Baldwin, B. S. and Lomax, H. 1978, "Thin Layer Approximation and Algebraic Model for Separated Turbulent Flows", AIAA Paper 78-257
- [14] Arnone, A., Carnevale, E., Marconcini, M., 1997, "Grid dependency study for the NASA rotor 37 compressor blade", Proceedings of ASME Turbo Expo 1997, 97-GT384
- [15] März, J., Hah, C., Neise, W., 2002, "An Experimental and Numerical Investigation into the Mechanisms of Rotating Instability", ASME Journal of Turbomachinery, 123, pp. 367-374
- [16] F. Rubecchini, M. Marconcini, M. Giovannini, J. Bellucci and A. Arnone, "Accounting for Unsteady Interaction in Transonic Stages," J. Eng. Gas Turbines Power, vol. 137, no. 5, pp. 052602-052602-9, 2015.
- [17] B. S. Baldwin and H. Lomax, "Thin Layer Approximation and Algebraic Model for Separated Turbulent Flows," AIAA Paper No. 78-257, 1978.
- [18] P. R. Spalart and S. R. Allmaras, "A One-equation Turbulence Model for Aerodynamic Flows," La Recherche Aéronautique, vol. 1, pp. 5-21, 1994.
- [19] D. C. Wilcox, Turbulence Modeling for CFD, 2nd ed., La Cañada, CA: DCW Industries Inc., 1998.
- [20] F. R. Menter, "Two-Equations Eddy Viscosity Turbulence Models for Engineering Applications," AIAA Journal, vol. 32, no. 8, p. 1598-1605, 1994.
- [21] W. W. Copenhaver, E. R. Mayhew, C. Hah and A. R. Wadia, "The Effect of Tip Clearance on a Swept Transonic Compressor Rotor," J. Turbomach., vol. 118, no. 2, pp. 230-239, 1996.
- [22] J. J. Adamczyk, M. L. Celestina and E. M. Greitzer, "The Role of Tip Clearance in High-Speed Fan Stall," J. Turbomach., vol. 115, no. 1, pp. 28-38, 1993.
- [23] L. Cozzi, F. Rubecchini, M. Marconcini, A. Arnone, P. Astrua, A. Schneider, A. Silingardi "Facing the challenges in CFD modelling of multistage axial compressors", Proceedings of ASME Turbo Expo 2017, GT2017-63240

APPENDIX – CFD SOLVER

The CFD solver used is the TRAF code ([16]) in its parallelized version. The numerical setup has been developed in the framework of the collaboration between Ansaldo Energia and the University of Florence. Further details on this numerical setup can be found in Cozzi et al. ([23]).

The space discretization is based on a cell-centred finite volume scheme. An artificial dissipation model is available in the code and to minimize the amount of artificial diffusion inside the shear layers, the terms are weighed with an eigenvalue scaling.

Several turbulence closures are implemented in TRAF code: the algebraic Baldwin–Lomax model [17], the Spalart–Allmaras one-equation model [18], the two-equation $k-\omega$ model developed by Wilcox [19] and Menter’s shear stress transport model [20].

One of the most challenging issues which arise in multistage axial compressor simulations is the need for being able to predict the stall margin with a certain level of accuracy with a steady-state analysis. Especially for compressors with a high stage count, due to mechanical issues, the rear and core stages tend to have high rotor tip gap. This leads to complex and unsteady 3D flow structures in the clearance region, especially throttling up the compressor towards the surge line. In this case a reliable stall margin prediction through steady-state simulations becomes even more demanding. Even if unsteady simulations could be an appropriate answer to these issues, the time and computational effort needed is currently not suitable for industrial design and design-validation purposes. To face the industrial need for a robust computational setup to run steady-state simulations of multistage axial compressors, the algebraic Baldwin-Lomax model has been chosen as turbulence closure between all the options available in the code. More complex one- and two-equation turbulence models have been tested on several geometries belonging to compressors already running on-site, leading to a significant underestimation of the stall margin. The numerical setup has been extensively validated on open literature test case and proprietary data (high-speed test on subsonic and transonic cascade, full-scale test bed measurements). An example of validation on Rotor 67 is reported in Figure 10.

Computational Grids, Boundary Conditions, mixing plane model and clearance model

Elliptic H-type grids with typical block dimensions of $141 \times 65 \times 81$ grid points in stream-wise, pitch-wise, and span-wise directions, respectively. The grid spacing has been chosen to obtain a y^+ value lower than 2.0. As far as boundary conditions are concerned, the radial distributions of total temperature, total pressure and flow angles are prescribed at the computational domain inlet, while the outgoing Riemann invariant is taken from the interior. On the domain outlet section, the static pressure span-wise distribution is enforced, while density and momentum components are extrapolated. Regarding the clearance model, the grid has been “pinched” in the tip region and a periodicity boundary condition between the two grid sides has been used. As far as concern the mixing planes, the non-reflecting model described in Cozzi et al. [23] has been used.

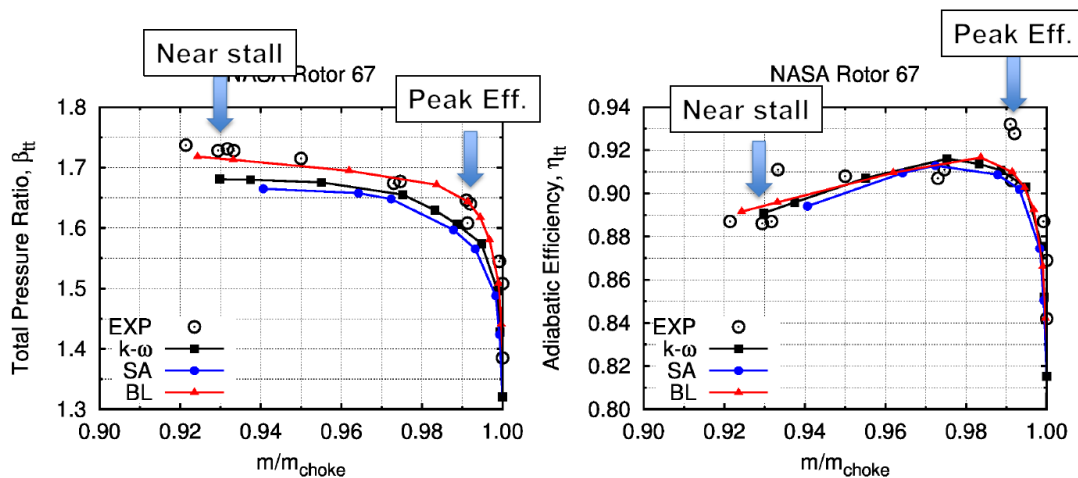


Figure 10: Numerical Setup validation on Rotor 67 test case. Turbulence model assessment, K-Omega, Spalart-Allmaras (SA) and Baldwin-Lomax (BL). (Marconcini M. and Rubecchini F., 2016)